DOSE FIELDS PRODUCED BY CONVERGENT IRRADIATION USING A NARROW PROTON BEAM

S.I. Blokhin, V.M. Breev, Ya.L. Klejnbok,
M.F. Lomanov, V.M. Narinskij, L.M. Pavlonskij,
V.I. Reznik, V.S. Khoroshkov, G.G. Shimchuk

Meditsinskaya Radiologiya, 19, No. 7, 50-56 (1974)

Translated at CERN by R. Luther
(Original: Russian)
Not revised by the Translation Service

(CERN Trans. Int. 76-1)

Geneva
December 1975

DOSE FIELDS PRODUCED BY CONVERGENT IRRADIATION USING A NARROW PROTON BEAM

Narrow beams of accelerated protons are being successfully used in the local irradiation of intracranial structures (K. Rollin, McCombs, Larsson, Chong et al.). The dose field set up by these beams is characterized by the sharp decrease of the dose at the edge of the target and the extremely low dose outside the irradiated volume. It is easy to reduce the beam loading on healthy tissue situated along the beam path when the radiation converges from many directions.

At the ITEP proton synchrotron (Moscow) a proton beam of up to 200 MeV with a dose rate of several thousand rad per minute (one 1.5 μsec pulse every 4 sec) has been developed and is being used for the treatment of oncological diseases in patients (V.S. Khoroshkov et al., S.I. Blokhin et al.). This paper describes the production of a narrow beam for the convergent irradiation of the hypophysis using the 'transmission' method and the measurements carried out on this beam.

When a 200 MeV beam is used, there is not much proton scattering in the tissue, and the dose distribution in the beam varies only slightly on its way from the surface of the body to the target. At the same time the background of secondary radiations produced by the interaction of the protons with the tissue and any shaping devices in the beam's path places healthy tissue at risk. This consideration has led us to seek the best possible system for producing the narrow beam and to devote considerable attention to the development of a universal method for measuring the proton beam and secondary radiation doses at the same time.

The system for producing the narrow proton beam consists of a series of collimators. The beam is first made slightly wider than necessary and is then reduced to the right dimension immediately before it enters the patient. With this system the primary collimators which absorb most of the protons and act as a source of undesirable secondary radiation are far enough away from the

patient and are concealed behind shielding. The large gap between each of the collimators arranged in series accurately determines the direction of the beam. The beam lay-out is shown in fig. 1. The collimator (1), hole 10 mm in diameter, is 4 m from the patient. A biological screen (2) with a collimator (3), hole 30 mm in diameter, is placed at the point where the beam leaves the vacuum channel. The rack (4) holds a collimator (5) and a mobile collimator (6) between which is placed an electromagnetic pick-up device for monitoring the beam. Collimator (5) ensures the preliminary shaping of the beam: after a number of experiments, which are described below, the ideal diameter of collimator (5) was found to be 1 mm less than that of collimator (6). Collimator (5) also shields the electromagnetic pick-up (7) against any penetrating radiation. The latter distorts the pick-up's readings considerably in narrow beams where the useful signal is weak. Owing to the scattering of the beam the electromagnetic pick-up (7) records a somewhat larger proton flux than present at the output of collimator (6). The appropriate correction is made by comparing the readings from pick-up (7) and from the induced activity detector placed in the position of the irradiated target in the tissue-equivalent phantom.

For absolute calibrations the induced activity method was used which has an accuracy of ± 5%. There is one interesting point about this method. In view of the fact that the production cross-section for radioactive carbon -C^{11}- and the energy losses of 50-200 MeV protons have the same energy dependence, this method may be used to determine correctly the contribution to the dose by the main part of the mixture of moderated protons produced when the beam is scattered on the collimator walls.

There are considerable difficulties involved in the measurement of the dose field of a narrow proton beam because good spatial resolution is required and also because the correct allowance has to be made for the contribution from scattered radiation which is particularly pronounced near the beam. The disadvantages of using the photodensitometric method for these measurements (A.S. Birdzh et al.) are the poor reproducibility and the dependence

of the readings on the radiation's composition and spectrum. The semiconductor detector used in static radiation fields (Kjellberg et al.) does not usually survive heavy doses of radiation and is not convenient for research into the volume dose fields produced by pulsed beams.

In order to measure the dose field produced by the transmission proton beam, we used a solid track detector (STD) consisting of a target of heavy fissile elements (U^{238} etc.) and a glass backing in which the fission fragments are detected. The special feature of this detector is that it can measure not only the distribution of the absorbed dose due to $>$ 100 MeV protons from the main beam but also the radiation dose caused by secondary fast and superfast neutrons whose relative contribution is accounted for in the detector readings (from U^{238} and certain other nuclei) with a factor close to the Q-factor (M.F. Lomanov et al.). At this stage it is advisable to use the Q-factor instead of RBE in therapeutic radiation because the data on RBE are not precise enough to allow an objective estimate of the radiation dose on critical organs. Thus, in accordance with the paper quoted, the STD is used to measure the combined proton and neutron dose equivalent directly in rem. It is known that other types of radiation which are only just picked up by this detector (thermal and intermediate neutrons, γ rays, multiply charged ions) make a relatively small contribution to the total dose.

The STD target consists of uranium foil or (for measuring the intensity distribution in the beam) bismuth sprayed on to a mica plate. The thickness of the spray coating is greater than the mean free path of the fission fragments ($\sim$ 6 μm). After the mica backing has been etched in a 3% solution of fluoric acid, traces of damage could be observed when magnified under a microscope 400 times. The resolution was 0.2 mm and the measurement accuracy $\pm$ 10%.

In order to gain a better understanding of the conditions surrounding the production of the narrow beam, measurements were made using the uranium STD at a depth of 75 mm inside a plastic tissue-equivalent phantom. Collimator (6) (viz fig. 1) 6 mm in

diameter was placed 50 mm from the specimen. Preliminary collimator (5) had diameters of 5 and 6 mm. The comparison of the dose distributions for these two collimator (5) diameters is shown in fig. 2. In the beam the radiation distributions virtually coincide, but the background surrounding the beam is $1\frac{1}{2}$ - 2 times greater when collimators (5) and (6) are the same size. This was the reason why the model with the enlarged exit collimator window was finally chosen. The measurements show that the dose drops sharply to 0.2% of the dose at the centre of the field at distances as short as 10-13 mm from the geometric edge of the beam (defined by the radius of the collimator).

In order to measure convergent radiation dose fields, a special tissue-equivalent phantom was developed and produced. It was attached to a rotary stereotaxic instrument used for irradiating hypophyses in patients (V.I. Abazov et al.). The tissue-equivalent phantom used for the measurements is made from mylar. A ring of tungsten wire 0.2 mm thick is attached to the centre of the phantom in order to bring the phantom in to line with the rotation axis for X-rays. The same sequence is followed when lining up the phantom as when the intracranial target in a patient is brought into line with the beam. It is possible to fit detectors along the beam axis inside the phantom. Up to six detectors may be installed in the phantom at any one time. One of these is usually placed in the central cross-section ($Z = 0$), and the others in cross-sections $Z = \pm 4, \pm 8, \pm 12, \pm 16, \pm 20, \pm 27, \pm 35$ mm. The Z axis corresponds to the centre line through the patient's temple and runs counter to the beam. When the detectors are placed in position, the following condition of tissue equivalence is met: the total depth (in grams per 1 cm^2) of the materials (glass backings and mylar) which the beam traverses on its way to the detector equals the distance (in centimetres) from the edge of the phantom to the point where the measurements are taken. The thickness of the glass corresponds to the thickness of the bone, and the thickness of the mylar and air gaps matches the depth of the tissue. The fragments emitted during the fission of heavy nuclei have some angular anisotropy. An investigation was therefore

made of the emission of fission fragments from bismuth nuclei as a function of the angle at which the proton beam strikes the detector. The angular dependence shown in fig. 3 is constant within the range of angles at which the hypophysis is irradiated. The small degree of anisotropy, which does not exceed 20% even in the case of omnidirectional radiation allows solid bismuth (1) detectors to be used for measurements in convergent exposures.

In order to obtain the dose fields produced by convergent radiation, the lateral intensity distributions are measured at different depths inside the phantom. With these data it is easy to obtain a picture of the isodoses in any plane by plotting graphs.

Fig. 4 is an example of the dose distribution in the convergent radiation field produced by an oval beam measuring 6 by 8 mm. The phantom was irradiated from 25 directions separated from one another by 7° and 6° in the vertical and horizontal planes respectively (fig. 5). Altogether 6 convergent radiation dose fields were produced and measured using round (6 and 7 mm in diameter) and oval (6 by 8 mm) beams from 25 and 20 directions respectively. For each field isodose maps are shown in two mutually perpendicular planes passing through the temple axis Z, and also the lateral dose distributions for cross-sections perpendicular to the Z axis and at various distances from the central cross-section (Z = 0). The X axis corresponds to the body's vertebral axis and the Y axis is aligned with the patient's occiput.

The measured dose distributions may be compared with the calculated values obtained by adding up the experimental fields of single-field irradiation (viz. fig. 2), the axes of which intersect at one point, and the angles of convergence coincide with the prescribed values. The results of the addition were compared with

---

(1) Detectors made from heavier elements have even better characteristics since the amount of anisotropy decreases as the atomic number increases.

the phantom's convergent radiation fields. The following field characteristics were revealed :

1. The distribution in the field's central cross-section coincides with the calculated value (fig. 6).

2. The distribution along the line of the temple deviates from the calculated value where the slope is steepest (fig. 7).

3. The dose equivalent at points away from the main area of radiation matches the calculated value (fig. 8).

The deviation from the calculated value observed along the Z axis, which is apparently due to the imprecise method of rotating the device, does not lead to any significant deterioration in the dose field.

With the convergent radiation, in each plane perpendicular to the Z axis, a reticular structure occurs, the inhomogeneity of which decreases as the centre of convergence is approached. The measurements showed that this inhomogeneity was not observed in the area of the target site itself. At cross-section Z = 16 mm the dose fluctuates as much as ± 20% about a mean value in the case of 25 fields. The percentage dose in this cross-section nowhere exceeds the dose on the beam axis which amounts to 9% (viz. fig. 7). Outside the region $Z < 20$ mm the percentage dose does not exceed 4% for 25 and 5% for 20 fields, which corresponds to the maximum dose produced by irradiation from every direction. Thus, for the given number of fields, the inhomogeneity in the central radiation area is such that the tolerance dose is not accidentally exceeded at specific points in the field.

The results of the measurements served as the basis for determining the topographical data used for the irradiation of hypophyses in a group of patients exposed to the ITEP proton beam in 1972.

Conclusions

1. A system is developed for producing a narrow proton beam (either with a round cross-section measuring 6-7 mm in diameter or with an oval cross-section measuring 6 by 8 mm) at an energy of 200 MeV for the purposes of convergent irradiation using 20-100 transmission fields. The beam is shaped by means of a system of collimators.

2. A high-sensitivity electromagnetic pick-up is developed for monitoring the beam and programming the dose. The absolute calibration of the dose is carried out by measuring the induced activity in carbon.

3. By using the solid track detector which records fission fragments from U^{238} and other heavy elements, it is possible to measure the dose distribution to a high degree of resolution ($\sim$ 0.2 mm) and accuracy $\pm$ 10% in the $1\text{-}10^6$ rem range. The detector gives the dose equivalent of mixed $>$ 100 MeV proton and $>$ 1 MeV neutron radiation up to an accuracy of 1.5 rad. The efficiency of the detector decreases with particles of lower energies, but this is not so important because these particles do not contribute much to the dose.

4. The dose fields for convergent radiation in a tissue-equivalent phantom are obtained and measured. The fields are characterized by a steep slope at the edge : the dose drops from 75% to 20% 5 mm along the temple line and 1.5 mm along the line perpendicular to it. It is thus possible to supply a high dose of massive radiation ($\sim$ 15000 rem) to the hypophysis without exceeding the tolerance dose in the critical structures adjacent to it - the chiasm and other cerebral nerves.

5. The dose equivalent received by the various critical organs of the head is low. In the case of a beam 6 mm in diameter in the central cross section perpendicular to the temple line, the dose drops to 1% of the target site dose at a distance of only 7 mm from the edge of the hypophysis and to 0.1% at a distance of 20 mm.

Bibliography

1. S.I. Blokhin, L.L. Gol'din, Ya. L. Klejnbok et al. Med. radiol., 1970, No. 5, p. 64.
2. M.F. Lomanov, G.G. Shimchuk, R.M. Yakovlev, Atomn. energiya, 1973, No. 3.
3. V.S. Khoroshkov, L.Z. Barabash, A.V. Barkhudaryan et al. Med. radiol., 1969, No. 4, p. 58.
4. A.S. Birdzh, Kh. O. Anger, S.A. Tobiash, in the book "Radiation dosimetry" edited by G. Hine, G. Brownell, New York 1956.
5. Y.L. Claude, Chong et al. Radiol. Clin, N. Amer., 1969, v. 7 p. 318.
6. R.H. Kjellberg et al. Trans. Amer. Neurol. Ass., 1962, v. 87, p. 216.
7. B. Larsson, Radiat. Res., 1967, Suppl. 7, p. 304.
8. K. Rollin, McCombs, Radiology, 1957, v. 68 p. 797.

Manuscript received on 18.6.1973.

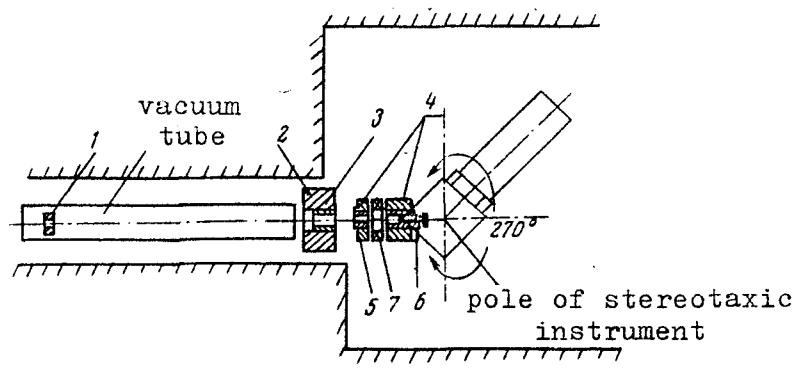

Figure 1. Layout of system for shaping a narrow beam. Explanations in the text.

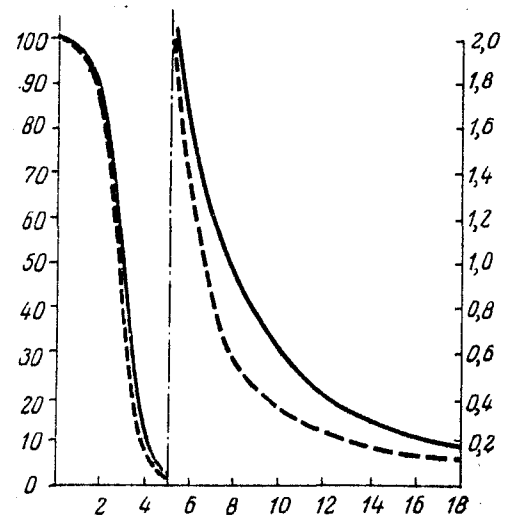

Figure 2. Intensity distribution in a ø 6 mm proton beam 75 mm inside a phantom.

Solid curve – collimators (5) and (6) are of the same diameter.
Dashed curve – diameter of collimator (5) 1 mm smaller.
Horizontal axis – distance from the centre of the beam (in mm)
Vertical axis – relative dose (in %).

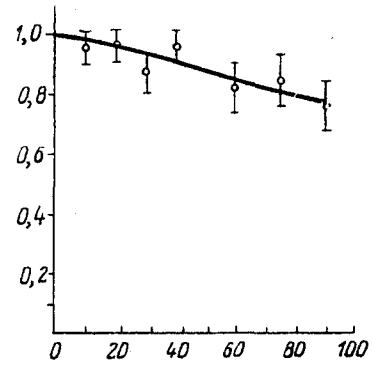

Figure 3. The yield of fission fragments for Bi as a function of the angle at which the proton beam strikes the detector.

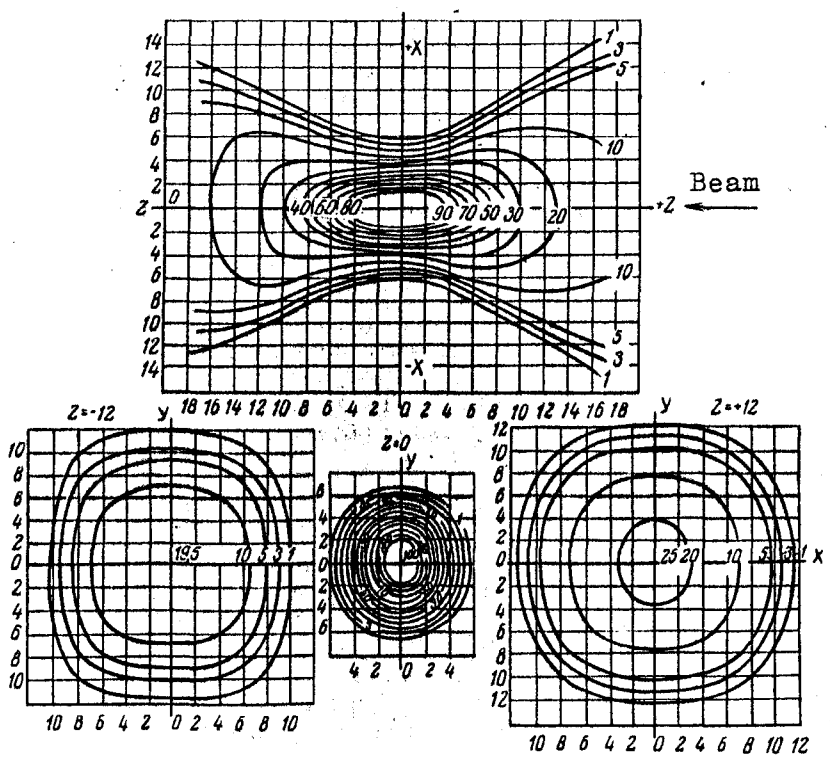

Figure 4. Dose distribution in the case of irradiation by a 6 x 8 mm^2 oval beam converging from 25 directions.

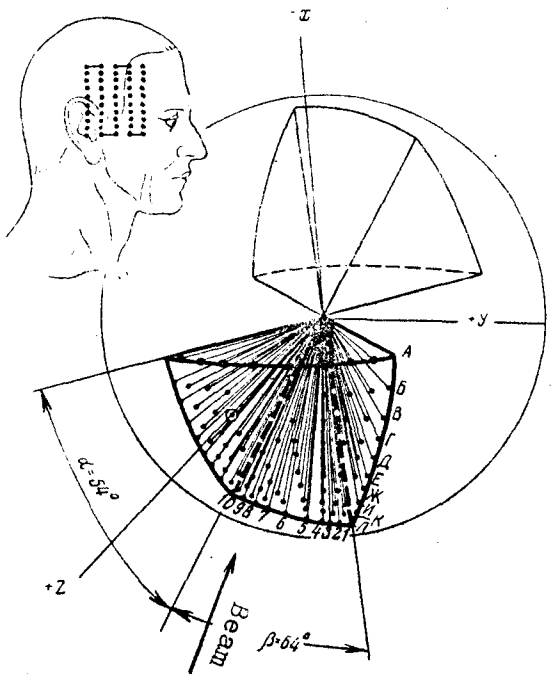

Figure 5. Geometry of convergent radiation.

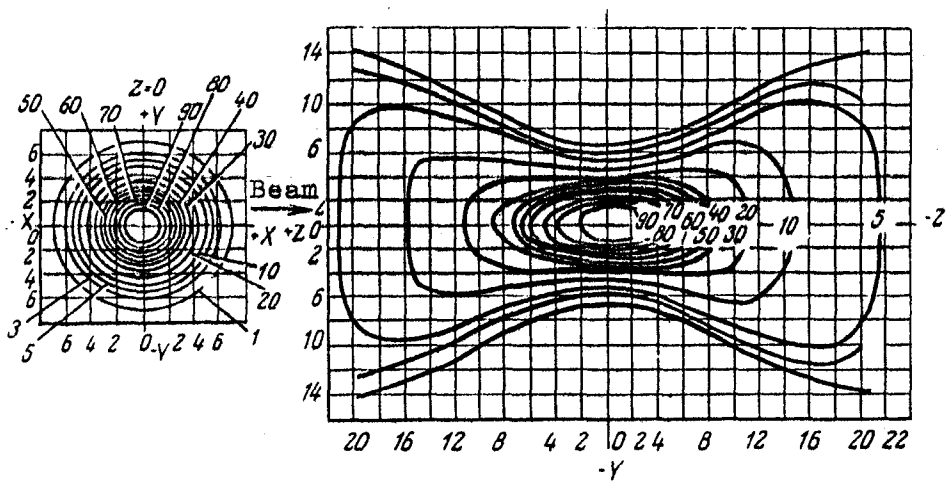

Figure 6. Isodose map showing irradiation of the hypophysis by a ø 6 mm round beam converging from 25 directions.

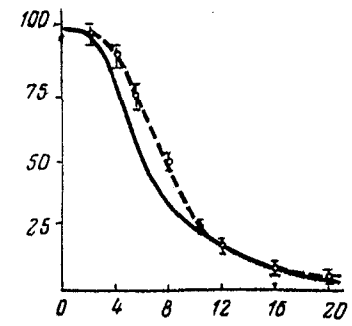

Figure 7. Dose distribution along the line of the temple. The solid line is the calculated curve, and the dashed line is the experimental result.

horizontal axis – Z (in mm)
vertical axis – dose along the Y-axis (in %).

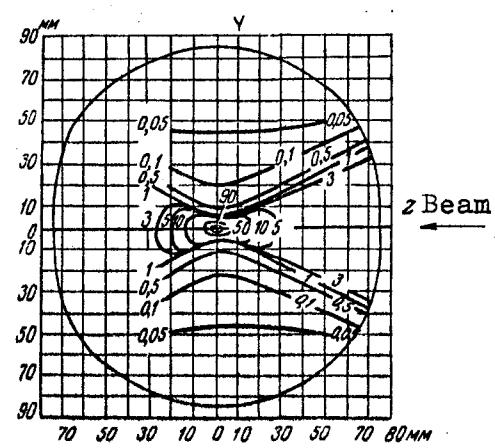

Figure 8. Distribution of dose equivalents outside the exposed area when the hypophysis is irradiated by a ø 6 mm round beam converging from 25 different directions.